

Reply to Reviewer #1:

General comments: This paper presents results from a study on the impact of climate variability on the rapid increase of winter haze pollution in northern China around 2011-2015. It is a well written paper on an important subject. The authors have posed a pivotal scientific question about the haze pollution in northern China, which can have a critical implication on the long-term trends of haze. In addition, the authors have addressed the scientific question effectively by using a nested-grid global photochemical model. **I believe that the paper deserves publication in ACP** provided that the following two specific comments are addressed.

1. (1) The main argument of the paper depends fundamentally on the validity of model simulations described in the “section 2.2 Geos-Chem description and experimental design”. It is essential that the performance of the model used to simulate haze pollution in North China is validated or at least evaluated against observations. Figure 1 of the paper could be used to some extent for evaluating the model performance, but additional simulations with historical emissions are needed.

(2) Judging from the trends of anthropogenic emissions, this reviewer is afraid that results from simulations with historical emissions might turn out to be significantly different from observed haze days. In any case, uncertainty in the model needs to be included in the discussions of sections 3-5.

Reply:

(1) We selected the year of 2015, which has just begun to strengthen emission reduction, and 2017, which has launched the air pollution prevention and management plan for “2+26” cities (Yin and Zhang, 2020), as two representative years to **simulate the actual PM_{2.5} concentration**, so as to evaluate the performance of the GEOS-Chem model. The emission factors and meteorological conditions of 2015 and 2017 were be used respectively to simulate the PM_{2.5} concentrations in early winters of 2015 and 2017. The simulation results are very **close to the observed data** in the two years (Figure S3) with high correlation coefficients reaching **0.88 and 0.85**, indicating that **the simulated data could basically reflect the change of actual PM_{2.5} concentrations**. We have added this part about the model evaluation in the Section 2.2, and added a new Figure S3.

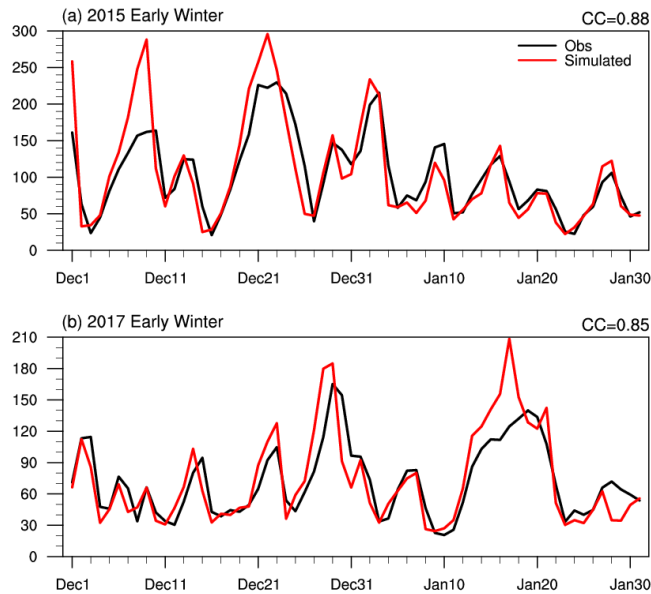


Figure S3. Temporal evolutions of observed (black) and simulated (red) PM_{2.5} concentrations (unit: $\mu\text{g m}^{-3}$; blue) in 2015 (a) and 2017 (b) early winter in North China.

In fact, the GEOS-Chem model has a **wide application**, and we have introduced **a few applications of others studies** in Section 2.2 to demonstrate the performance of the model laterally.

(2) Our simulations were designed to **emphasize the effects of climate**, so we used fixed emissions. In addition to the experiments with fixed emission in 2010, **a new set of experiments** was carried out by GEOS-Chem with **fixed emissions in 1985**, representing a low emission level. This simulation of the frequency of haze days ($>50 \mu\text{g m}^{-3}$) also **reproduced the trend reversal of haze pollution very well (Figure R1)**, **similarly with the observed haze days.**

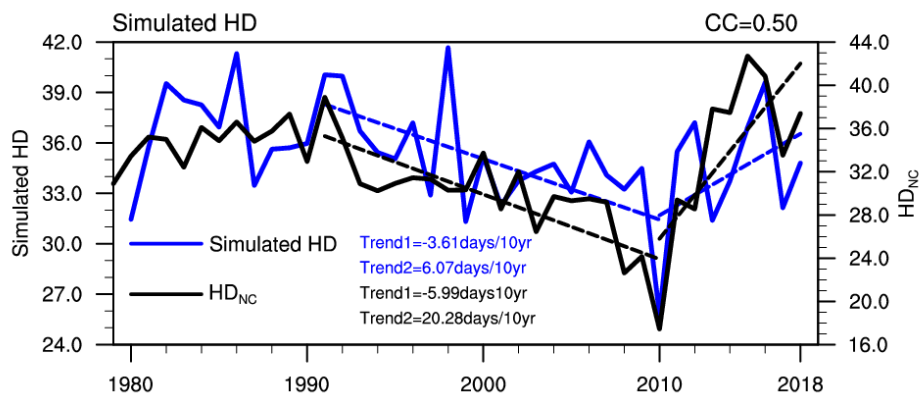


Figure R1. Temporal evolutions of HD_{NC} (in black), simulated haze days under 1985 (unit: days; blue) emission scenarios in NC. The dashed lines denote linear regressions for 1991–2010 (P1) and

2010–2018 (P2). The black and blue Trend 1 and Trend 2 represent the linear trends of the observed and simulated haze days 1985 emission scenarios in P1 and P2, respectively.

Considering the change of anthropogenic emission, in Dang and Liao’s finding (2019), the CTRL experiment (black line in Figure R2a) also **showed a decreased trend during 1985 to 2002** (blue grids in Figure R2b) and **an increased trend after 2010** (red grids in Figure R2b). Although this trend is weaker than the MET experiment, which only considered the effects of meteorological conditions (green line R2a), the overall change of trend in the CTRL experiment is **consistent with observations**. And Mao L. et al. (2019, National Science Review) also raised the **contradiction between the change of anthropogenic emissions and haze days** based on an observation approach, which was manifested as the number of winter haze days with no significant trend in most provinces and districts in eastern China from 1973 to 2012, contrary to the 2.5-fold increase in the emissions of particulate matter and its precursors (PM emissions) in the same period of time. And we have **added the discussion of the uncertainties** in section 5.

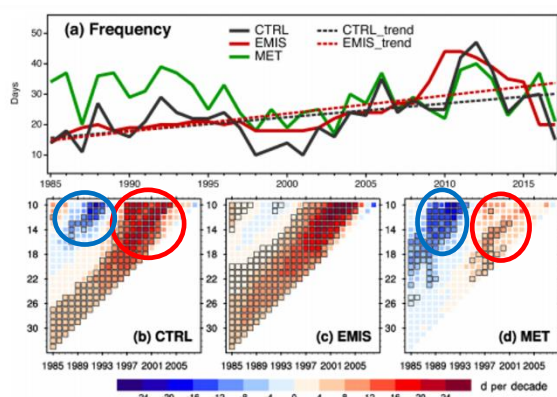


Figure 10. (a) Time series of frequencies (days) of regional SWHD in BTH from three simulations (CTRL, EMIS, MET) for 1985 to 2017. (b–e) Time series of linear trends calculated over different periods for simulated frequencies of the (b) CTRL, (c) EMIS, and (d) MET simulations. The x axis indicates the start year, and the y axis indicates the number of years since the start year during which period the trend is calculated. The filled color in each square shows the calculated trend value, and those values marked with black borders are significant above the 95% confidence level.

1. CTRL is the control simulation with variations in meteorological parameters, anthropogenic emissions, and biomass burning emissions from 1985 to 2017.
2. EMIS is the simulation with changes in anthropogenic and biomass burning emissions over 1985–2017, while the meteorological fields were fixed at the 1985 levels. The aim of this simulation is to quantify the impacts of changes in emissions on SWHDs during 1985–2017.
3. MET is the simulation with changes in meteorological fields over 1985–2017, while anthropogenic and biomass burning emissions were fixed at the 2015 levels. This simulation is set to examine the impacts of changes in meteorological parameters on SWHDs during 1985–2017.

Figure R2. A key figure and design of three numerical experiments in *Dang and Liao (2019)* published in *Atmos. Chem. Phys.*

Related references:

Yin, Z., and Zhang, Y.: Climate anomalies contributed to the rebound of PM_{2.5} in winter 2018 under intensified regional air pollution preventions, *Sci. Total Environ.*,

726, 138514, 2020.

Dang, R. and Liao, H.: Severe winter haze days in the Beijing–Tianjin–Hebei region from 1985 to 2017 and the roles of anthropogenic emissions and meteorology, *Atmos. Chem. Phys.*, 19, 10801–10816, <https://doi.org/10.5194/acp-19-10801-2019>, 2019.

Mao, L., Liu, R., Liao, W., Wang, X., Shao, M., Liu, S. and Zhang, Y.: An observation-based perspective of winter haze days in four major polluted regions of China. *National Science Review*, 6, 515–523, doi: 10.1093/nsr/nwy118, 2019.

Revisions:

Lines 79-85: At present, GEOS-Chem model has been widely used, Dang et al. (2019) showed that the simulated spatial patterns and daily variations of winter PM_{2.5} based on this model agree well with the observations from 2013 to 2017, available years with measured PM_{2.5}. We selected the year of 2015, which has just begun to strengthen emission reduction, and 2017, which has launched the air pollution prevention and management plan for “2+26” cities (Yin and Zhang, 2020), as two representative years to simulate the actual PM_{2.5} concentrations, so as to evaluate the performance of the GEOS-Chem model. The simulation results are very close to the observed data (Fig. S3) with high correlation coefficients reaching 0.88 and 0.85 in 2015 and 2017, indicating this model could basically reflect the change of actual PM_{2.5} concentrations.

Lines 278-282: Note that a number of factors contribute to the uncertainties in our results. Although a high emission scenario was used to simulate the number of haze days and emphasized the influence of meteorology, no complete and varied emission inventories were used to drive the GEOS-Chem model to make a comparison, which caused certain uncertainty. Furthermore, when assessing the contribution percentages of the external forcing factors, the coupling effect between climate variability and anthropogenic emissions was not considered, therefore the contribution rate of climate conditions might be overestimated.

2. “The autumn SST in the Pacific and Atlantic, Eurasian snow cover and central Siberian soil moisture, which exhibited completely opposite trends before and after 2010, were proven to stimulate identical trends of meteorological conditions related to haze pollution in North China.” in the abstract and conclusion section

maybe an overstatement, at least in terms of the relatively large uncertainty of the model. A more fundamental concern is that the method used in evaluating contributions of the four climate drivers does not imply any causal relationship.

Reply:

We have adopted a **more rigorous statement** to explain the effect of the four external forcing factors on haze events in abstract and conclusion section.

Revisions:

Lines 14-16: The autumn SST in the Pacific and Atlantic, Eurasian snow cover and central Siberian soil moisture, which exhibited completely opposite trends before and after 2010, might had close relationships with the identical trends of meteorological conditions related to haze pollution in North China

Lines 267-269: In this study, the external forcing factors that closely related to the significant growth of HD_{NC} after 2010 and the associated physical mechanisms were investigated. These factors might strongly linked to the anomalous anticyclone over NC via exciting the EA/WR teleconnection pattern.....

Reply to Reviewer #2:

General comments: The authors proposed a very interesting question that haze pollution in early winter in North China experienced a rapid increase from 2010 after a two-decade decrease. This notion is supported by long-term haze days defined by visibility and relative humidity. By using model simulation and statistical analysis, they argued that climate variability is the dominant driver for rapid increase after 2010. They further analyzed the possible external climate forcings to support their conclusions. Overall, **the topic of this study fits this journal well**. The authors conducted modeling and statistical efforts to defend their conclusions. **I think it is publishable** before some concerns in the following are addressed.

1. I am most concerned about the rapid increase trend after 2010, because it looks like the trend is mainly driven by an extreme anomaly in 2010. As for visibility-based haze days, year 2010 doesn't change the increasing trend. But, I think the increasing trend will not hold for observed PM2.5 and simulated haze days if year 2010 is removed. If this is the case, that means the authors should take caution stating that there is rapid increase of haze pollution after 2010. It is better to focus on the long-term trend than only highlight the rapid increase after 2010. Other PM2.5-related measurements (e.g., satellite AOD) might be helpful.

Reply:

Many recent studies have focused on the **long-term trend in the haze problem and shown that might be driven by human activities and global warming** (Li et al, 2018; Yang et al, 2016; Horton et al, 2014; Cai et al., 2017). However, none of the above studies focused on the change in the haze trend. Therefore, our study is to **novelly focus on the trend reversal of HD_{NC} around 2010, which had stage inconsistencies with the trend of emissions and global warning**, and to explain the reasons from the perspective of climate change, which is the innovation of this work.

(1) We **excluded the extreme anomaly in 2010** and selected two periods from 1991 to 2009 and from 2011 to 2018 respectively to focus on the trend changes, so as to **further confirm the existence of the rapid increase after 2010**. We can be sure that the **trend reversal still exists and has not changed by removing year 2010**. In the two periods removing 2010, HD_{NC} also showed slowly decreased during 1991–2009

(P1) with a rate of **3.82 days/10 yr** but rapidly increased during 2011–2018 (P2) with a rate of **20.76 days/10 yr**, and both passed the 95% t test.

(2) The number of haze days calculated **using observed data** in Beijing from the US embassy (available from 2009 to 2016) also showed **an increasing trend without 2010** (Figure R1), with a rate of 2.3days/10yr and 6.0days/10yr when exceeding $75 \mu\text{g m}^{-3}$ and $100 \mu\text{g m}^{-3}$, respectively. The AOD data is monthly average, so it could not calculate the number of polluted days and cannot make comparison with HD_{NC} .

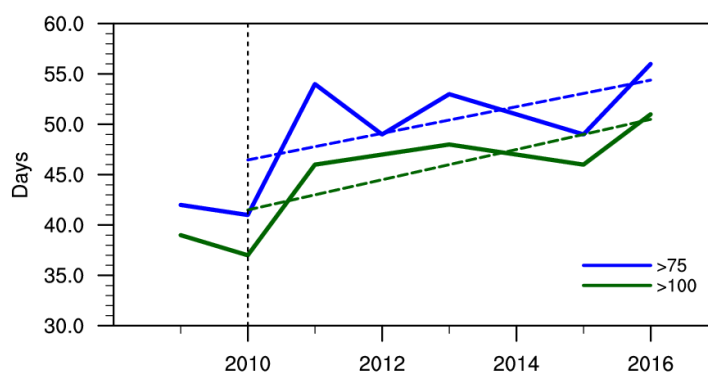


Figure R1. The number of days when the hourly $\text{PM}_{2.5}$ concentrations in a day exceeded $75 \mu\text{g m}^{-3}$ (blue) and $100 \mu\text{g m}^{-3}$ (green), respectively, from 2009 to 2016 using Beijing observed data from the US embassy. The dash lines represent the trends during 2010-2016.

(3) We also check a lot of previous studies, and can show you many **hard evidences** that the **trend reversal is reliable**. Many **observation-based researches also showed the same trend as ours**. Here, I summarized a part of them (independent researches and irrelevant with us) to show the **consistency** with our results. Actually, recent studies generally revealed that the boreal winter haze days across North China **had a trend reversal in 2010**, which is consistent with the result in our research (Shi et al., 2019; Mao et al., 2019). As the most polluted area in North China, Beijing-Tianjing-Hebei (BTH) region had a **statistically significant decline trend** of haze days during 1990-2010 (Figure R2; purple arrow), and a **rapid increase trend after 2010** (Figures R2; red arrow).

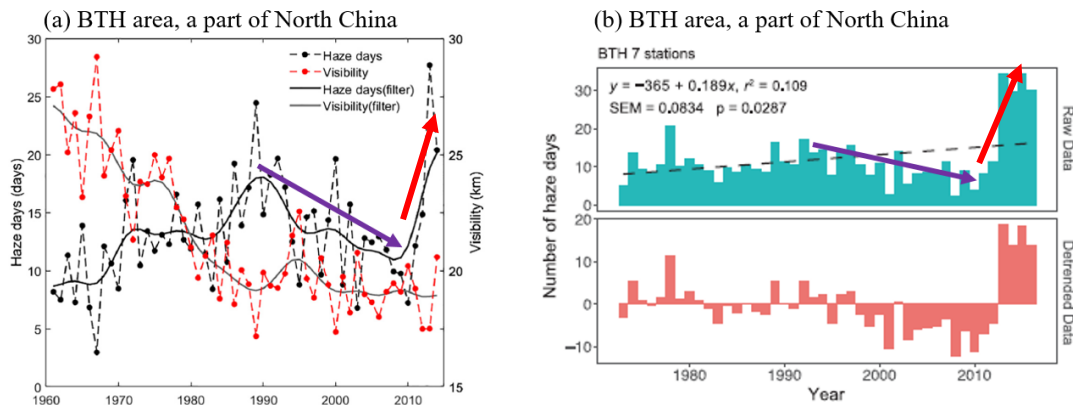


Figure R2. Variation of HD revealed by other researchers, the purple arrows indicate the trend approximately from 1990 to 2010, and the red arrows indicate the trend after 2010. (a) Mean winter haze days (black dashed lines) and visibility (red dashed lines) in the Beijing-Tianjin-Hebei (BTH) region (the most polluted area in North China) for 1961–2014. A 15-year low-pass Gaussian filter is drawn with solid lines. *This panel (a) was extracted from Shi et al., (2019) published on Atmospheric Research.* (b) HD in North China during the period 1973–2016. Absolute values are shown in blue, detrended values in red. Dashed lines denote linear regressions. *This panel (b) was extracted from Mao et al., (2019) published on National Science Review.*

(4) In 2017, the number of haze days decreased significantly, which was caused by the enhanced “2+26” emission reduction measures and the cold winter. However, this **did not affect the increased trend** after 2010. And in 2018, due to adverse meteorological conditions, even under strong emission reduction, PM_{2.5} concentration had a significant rebound (Yin and Zhang, 2020).

Related References:

Li, K., Liao, H., Cai, W., Yang, Y.: Attribution of anthropogenic influence on atmospheric patterns conducive to recent most severe haze over eastern China, *Geophys. Res. Lett.*, 45(4), 2072–2081, doi:10.1002/2017GL076570, 2018.

Yang, Y., Liao, H., Lou, S.: Increase in winter haze over eastern China in recent decades: Roles of variations in meteorological parameters and anthropogenic emissions, *J. Geophys. Res. Atmos.*, 121: 13050–13065, 2016.

Horton, D., Skinner, C., Singh, D., Diffenbaugh, N.: Occurrence and persistence of future atmospheric stagnation events, *Nat. Clim. Change*, 4, 698–703, 2014.

Cai, W., Li, K., Liao, H., Wang, H., and Wu, L.: Weather conditions conducive to Beijing severe haze more frequent under climate change, *Nat Clim Change*, 7, 257–262,

2017.

Shi, P., Zhang, G., Kong, F., Chen, D., Cesar Azorin-Molina, Jose A. Guijarro: Variability of winter haze over the Beijing-Tianjin-Hebei region tied to wind speed in the lower troposphere and particulate sources. *Atmospheric Research*, **215**, 1–11, 2019.

Mao, L., Liu, R., Liao, W., Wang, X., Shao, M., Liu, S. and Zhang, Y.: An observation-based perspective of winter haze days in four major polluted regions of China. *National Science Review*, **6**, 515–523, doi: 10.1093/nsr/nwy118, 2019.

Yin, Z., and Zhang, Y.: Climate anomalies contributed to the rebound of PM_{2.5} in winter 2018 under intensified regional air pollution preventions, *Sci. Total Environ.*, **726**, 138514, 2020.

Revisions:

Lines 112-114: Excluding year 2010 did not affect the change in the trend of the two periods, with a decreased rate of 3.82 days/10 yr during 1991–2009, and an increased rate of 20.76 days/10 yr during 2011–2018 (passing 95% t test).....

2. It is surprised that the simulations with fixed anthropogenic emissions can produce the observed reversal frequency of haze days very well. You also cite Dang and Liao (2019) to support this argument. I take a look at this reference, but I think their results didn't show an increasing trend after 2010.

I am very curious about if the role of anthropogenic emissions is very limited after 2010.

Reply:

In addition to the experiments with fixed emission in 2010, **a new set of experiments** was carried out by GEOS-Chem to **further enhance the reliability of the simulation**. The new simulation had changing meteorological fields in winter from 1980 to 2018 but the **fixed emissions in 1985** representing a low emission level. This simulation of the frequency of haze days ($>50 \mu\text{g m}^{-3}$) also **reproduced the trend reversal of haze pollution very well** (Figure R3). The simulation results are highly correlated with HD_{NC} and show a rapid increase after 2010. Therefore, the simulation results **can well reproduce the trend reversal of haze days** in both high and low emission levels, indicating that the **simulations are reliable and the rapid growth of haze after 2010 exists**.

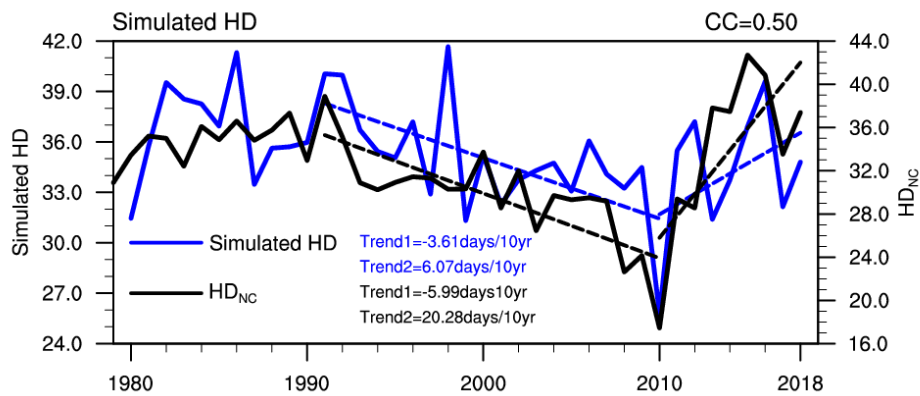


Figure R3. Temporal evolutions of HD_{NC} (in black), simulated haze days under 1985 (unit: days; blue) emission scenarios in NC. The dashed lines denote linear regressions for 1991–2010 (P1) and 2010–2018 (P2). The black and blue Trend 1 and Trend 2 represent the linear trends of the observed and simulated haze days 1985 emission scenarios in P1 and P2, respectively.

In Dang and Liao’s study, the definition of serious haze day is a day with daily mean $PM_{2.5}$ concentration exceeding $150 \mu g m^{-3}$, but in our study, it is exceeding $75 \mu g m^{-3}$. Therefore, we differ in the results of the change of trend. In the MET experiment, the increased trend is clear (Figure R4a, green line and red grid). This increasing trend is **more pronounced through a 9-year weighted moving average method** (Figure R4b). When considering changes in anthropogenic emission, that is, CTRL experiments, the **decreased trend during 1990-2010 was weaker** than in the MET experiment, which only considered the effect of meteorology. On the basis of the meteorological effect that caused haze decreased in P1 and haze increased in P2, a **continuous rising effect of emission** was superimposed. Both of them jointly lead to a **weakened decreased in P1 and a rapid increase in P2**. When assessing the contribution percentages of the external forcing factors, **the coupling effect between climate and emissions was not considered**, therefore the contribution rate of climate conditions might be **overestimated**. We have **added the discussion of this uncertainty** in section 5. For the long-term trend of haze, human activities are the **recognized and fundamental driver** (Li et al., 2018; Yang et al 2016). In our study, we focused on the trend reversal of **early stage decrease and later increase**, and explained it from a climate perspective.

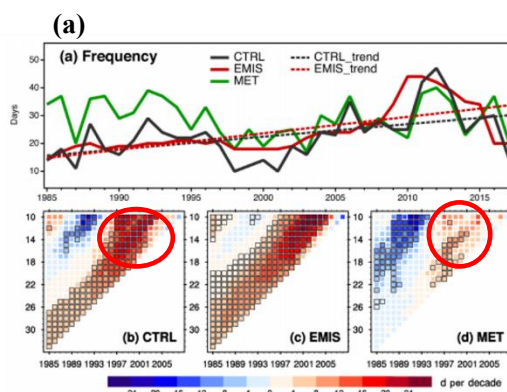


Figure 10. (a) Time series of frequencies (days) of regional SWHD in BTH from three simulations (CTRL, EMIS, MET) for 1985 to 2017. (b–e) Time series of linear trends calculated over different periods for simulated frequencies of the (b) CTRL, (c) EMIS, and (d) MET simulations. The x axis indicates the start year, and the y axis indicates the number of years since the start year during which period the trend is calculated. The filled color in each square shows the calculated trend value, and those values marked with black borders are significant above the 95 % confidence level.

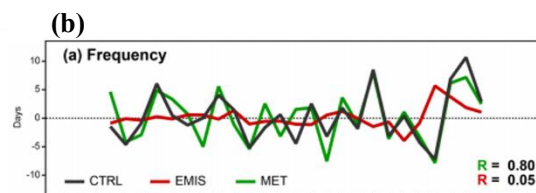


Figure 12. Interannual variations in SWHD (a) frequencies (days)

Figure R4. Key figures in *Dang and Liao (2019) published in Atmos. Chem. Phys.*, including Figure 10 and 12.

Related references:

Dang, R. and Liao, H.: Severe winter haze days in the Beijing–Tianjin–Hebei region from 1985 to 2017 and the roles of anthropogenic emissions and meteorology, *Atmos. Chem. Phys.*, 19, 10801–10816, <https://doi.org/10.5194/acp-19-10801-2019>, 2019.

Li, K., Liao, H., Cai, W., Yang, Y.: Attribution of anthropogenic influence on atmospheric patterns conducive to recent most severe haze over eastern China, *Geophys. Res. Lett.*, 45(4), 2072–2081, doi:10.1002/2017GL076570, 2018.

Yang, Y., Liao, H., Lou, S.: Increase in winter haze over eastern China in recent decades: Roles of variations in meteorological parameters and anthropogenic emissions, *J. Geophys. Res. Atmos.*, 121: 13050–13065, 2016.

Revisions:

Lines 281-282: Furthermore, when assessing the contribution percentages of the external forcing factors, the coupling effect between climate and emissions was not considered, therefore the contribution rate of climate conditions might be overestimated.

Line 283: For the long-term trend of haze, human activities are the recognized and fundamental driver (Li et al., 2018; Yang et al 2016).

Specific comments:

Title: The authors focused on “early winter” in this study, but you failed to define what’s “early winter”, December and January? Please clarify this in the title and also in the main text. Also, I am not sure if the conclusions support the “rapid increase” after 2010.

Reply:

In our study, the early winter is mean December and January. We further clarify that we focus on the trend change of haze in early winter in the title, and added the definition of early winter in the main text.

Revisions:

Line 1: Roles of Climate Variability on the Rapid Increases of Early Winter Haze Pollution in North China after 2010

Line 11:The number of haze days in early winter (December and January) in North China increased rapidly after 2010 but declined slowly before 2010,.....

Line 107:The number of haze days in early winter (December and January) in North China (HD_{NC}) reached a remarkable inflection point in 2010.....

Line19: You mentioned “human emissions” started to decline in mid-2000s. How did they jointly lead to rapid increase in haze days?

Reply:

It is true that human emissions have been reduced since mid-2000s, but **the pollution emissions still far exceed the capacity of atmospheric environment**, so it can **provide adequate particulate emissions** at all times to form haze pollution. This also contributes to the fact that haze pollution is extremely **sensitive** to meteorological conditions.

In February 2020, **the Ministry of Ecology and Environment** published an article focusing on the recent heavy air pollution in the Beijing-Tianjin-Hebei region and surrounding areas, with five experts explain the causes of the pollution **during COVID-19** **quarantines**

(http://www.mee.gov.cn/xxgk2018/xxgk/xxgk15/202002/t20200211_762584.html).

Zifa Wang, a researcher at the Institute of Atmospheric Physics of the Chinese Academy of Sciences, explained that pollution emissions have fallen, but **not by nearly as much**

as the environmental capacity. Although social activities are at a low level, pollutant emissions are **still more than twice the environmental capacity.** Kebin He also said that under the current emissions intensity of the “2+26” region, although the total emissions are reduces, most of the pollutant emissions accumulated to the few city, **making the load of the atmospheric pollutants in several cities far exceeds the environmental capacity and causing heavy pollution,** such as Beijing, Tianjin and other cities. At the current level of emissions reduction, pollutants still exceed the capacity of the atmosphere, especially in adverse meteorological conditions. So anthropogenic emissions and climate factors jointly lead to rapid increase in haze days after 2010.

Line 91: MLR should spell out.

Reply:

We have added the full spelling of MLR to the text.

Revisions:

Line 98: In this study, the statistical model of fitted HD_{NC} was built based on Multiple Linear Regression (MLR).

Line 102: The trend should be given with its statistical significance. Please check throughout the text.

Reply:

We have calculated a t test for trends, and given the statistical significance in the text.

Revisions:

Line 110: The trend of HD_{NC} was vastly different before and after 2010: slowly decreased during 1991–2010 (P1) with a rate of 4.67 days/10 yr but rapidly increased after 2010 (P2, 2010–2018) with a rate of 25.43 days/10 yr, both of them passing 95% t test.

Line 177-179: Thus, the persistent decline in SST_P during P1 (at a significant rate of -0.2 °C/10 yr, passing 95% t test; Table 1) contributed to the slowly decreasing trend of HD_{NC} (Fig. 4a) via the modulations of SST_P on the atmospheric circulation (Fig. S5).

During P2, the larger increase in SST_P at a rate of 2.0 °C/10 yr (passing 95% t test) dramatically drove the rapid increase in HD_{NC}.

Lines 193-194: The SST_A reached a inflection point in 2010 (Fig. 4b) and contributed to the falling of HD_{NC} during P1 (change rate of SST_A = 0.55 °C/10 yr, passing 95% t test) and the rising of HD_{NC} during P2 (change rate of SST_A = -0.52 °C/10 yr, passing 95% t test).

Lines 207-208: The Snowc index fell slowly until 2010 (with a rate of -1.8%/10 yr, passing 95% t test) and then rose rapidly (with a rate of 28.3%/10 yr, , passing 95% t test) and experienced a large trend reversal in 2010.....

Lines 220-221: The change rate of Soilw was 38.8 mm/10 yr passing 95% t test (opposite that of HD_{NC}) during P1, and the rate of change became more intense (-51.8 mm/10 yr, passing 95% t test) during P2.....

Lines 253-254: More importantly, the fitted curve revealed a decreasing trend of HD_{NC} (-5.24 days/10 yr, passing 95% t test).....

Lines 109-110: Only PM_{2.5} data in Beijing used from the national measurement network? Or PM_{2.5} over North China? This should be also clarified in the caption of Figure 1.

Reply:

The PM_{2.5} concentration **over North China** were used from the national measurement network, we have clarified both in the text and the caption of Figure 1.

Revisions:

Line 119:and the PM_{2.5} concentrations over North China monitored by China National Environmental Monitoring Centre from 2014 to 2018

Line 420-422: Figure 1.The blue and green solid (dashed) lines indicate the number of days when the hourly PM_{2.5} concentrations in a day exceeded 75 µg m⁻³ and 100 µg m⁻³, respectively, from 2009 to 2016 (2014 to 2018) using Beijing (North China) observed data from the US embassy (China National Environmental Monitoring Centre).....

Lines 136-137: I think they also show results with varying meteorology?

Reply:

We have added the analysis of their results with varying meteorology in the text.

Revision:

Lines 146-147: The GEOS-Chem simulations with changing emissions and fixed meteorological conditions failed to reproduce the change trend of haze (Dang and Liao, 2019), but with varying meteorology and fixed emissions could recognize the interannual variation of haze days.

Figure 1a: missing legend for green dash line. I don't think it is reasonable to show the red dash line. The sum of these pollutant emissions doesn't make sense.
Figure 1b: You should give observed trends of haze days along with the simulated trends.

Reply:

In Figure 1a, we have added the legends for blue and green dash lines, and removed the red dash line representing the sum of these pollutant emissions. And we have added the observed trends of haze days in Figure 1b.

Revision:

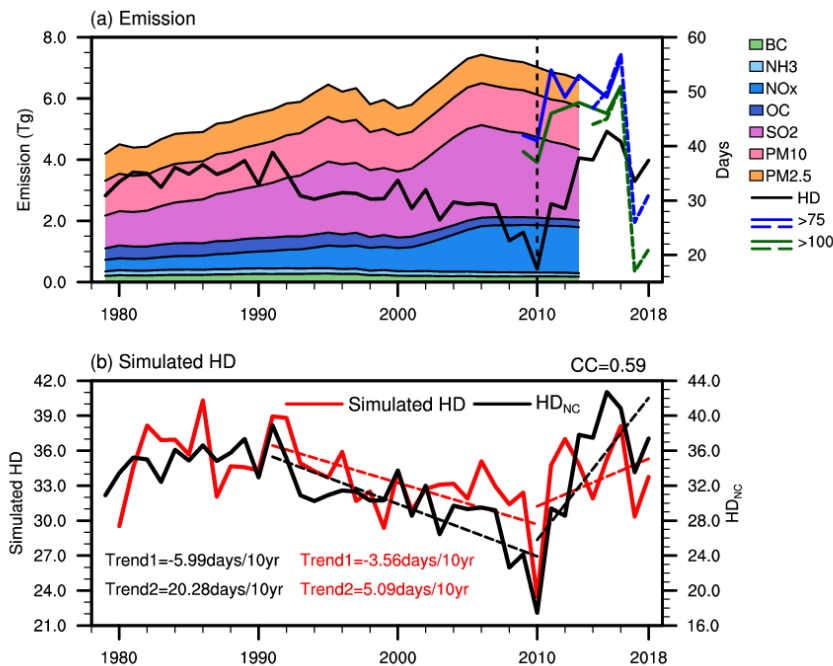


Figure 1. (a) Variations in the December-January emissions (unit: Tg) of black carbon (BC), ammonia (NH₃), nitrogen oxide (NO_x), organic carbon (OC), sulfur dioxide (SO₂), PM₁₀ and PM_{2.5} over North China from 1979 to 2013 and the variation in HD_{NC} from 1979 to 2018 (black solid line). The blue and green solid (dashed) lines indicate the number of days when the hourly PM_{2.5} concentrations in a day

exceeded $75 \mu\text{g m}^{-3}$ and $100 \mu\text{g m}^{-3}$, respectively, from 2009 to 2016 (2014 to 2018) using Beijing (North China) observed data from the US embassy (China National Environmental Monitoring Centre). (b) Temporal evolutions of HD_{NC} (in black), simulated haze days (unit: days; red) in NC. The dashed lines denote linear regressions for 1991–2010 (P1) and 2010–2018 (P2). The black and red Trend 1 and Trend 2 represent the linear trends of the observed and simulated haze days in P1 and P2, respectively.

Roles of Climate Variability on the Rapid Increases of Early Winter Haze Pollution in North China after 2010

Yijia Zhang¹, Zhicong Yin^{123*}, Huijun Wang¹²³

¹Key Laboratory of Meteorological Disaster, Ministry of Education / Joint International Research Laboratory of Climate and Environment Change (ILCEC) / Collaborative Innovation Centre on Forecast and Evaluation of Meteorological Disasters (CIC-FEMD), Nanjing University of Information Science & Technology, Nanjing 210044, China

²Southern Marine Science and Engineering Guangdong Laboratory (Zhuhai), Zhuhai, China

³Nansen-Zhu International Research Centre, Institute of Atmospheric Physics, Chinese Academy of Sciences, Beijing, China

Correspondence to: Zhicong Yin (yinzhc@163.com)

Abstract. North China experiences severe haze pollution in early winter, resulting in many premature deaths and considerable economic losses. The number of haze days in early winter (December and January) in North China (HD_{NC}) increased rapidly after 2010 but declined slowly before 2010, reflecting a trend reversal. Global warming and emissions were two fundamental drivers of the long-term increasing trend of haze, but no studies have focused on this trend reversal. The autumn SST in the Pacific and Atlantic, Eurasian snow cover and central Siberian soil moisture, which exhibited completely opposite trends before and after 2010, ~~were proven to~~ might had close relationships with stimulate identical trends of meteorological conditions related to haze pollution in North China. Numerical experiments with a fixed emission level confirmed the physical relationships between the climate drivers and HD_{NC} during both decreasing and increasing periods. These external drivers induced a larger decreasing trend of HD_{NC} than the observations, and combined with the persistently increasing trend of anthropogenic emissions, resulted in a realistic slowly decreasing trend. However, after 2010, the increasing trends driven by these climate drivers and human emissions jointly led to a rapid increase in HD_{NC} .

Keywords: haze, $PM_{2.5}$, trend reversal, anthropogenic emission, climate variability

1 Introduction

Haze pollution, characterized by low visibility and a high concentration of fine particulate matter ($PM_{2.5}$), has become a serious environmental and social problem in China, as haze dramatically endangers human health, ecological sustainability and economic development (Ding and Liu, 2014; Wang and Chen, 2016). Exposure to $PM_{2.5}$ was estimated to cause 4.2 million premature deaths worldwide in 2015 (Cohen et al., 2017), and in China, $PM_{2.5}$ caused up to 0.96 million premature mortalities in 2017 (Lu et al., 2019). Air pollution accounts for a loss of 1.2–3.8% of the gross national product (GNP) annually (Zhang and Crooks, 2012). The most polluted areas in China are North China (NC; 34–42°N, 114–120°E), Fenwei Plain, Sichuan Basin and Yangtze River Delta; among them, NC is the most polluted (Yin et al., 2015). Meteorological conditions characterized by low surface wind speeds and a shallow boundary layer result in stagnant air, which limits the horizontal and

31 vertical dispersion of particles and induces the accumulation of pollutants (Niu et al., 2010; Wu et al., 2017; Shi et al., 2019).
32 High relative humidity favors the hygroscopic growth of pollutants (Ding and Liu, 2014; Yin et al., 2015), and anomalous
33 ascending motions weaken the downward invasion of cold and clear air from high altitudes (Zhong et al., 2019). The
34 forecasting of meteorological conditions is more accurate on the synoptic scale, but the predictions of interannual variations
35 are not good enough. Thus, the prediction of haze is a considerable challenge.

36 Previous studies proved that the interannual to decadal variations in winter haze have strong responses to external forcing
37 factors, such as the sea surface temperature (SST) in the Pacific and Atlantic, snow cover and soil moisture (Xiao et al., 2015;
38 Yin and Wang, 2016a, b; Zou et al., 2017). Anomalies of these factors exerted their impacts to modulate local dispersion
39 conditions by atmospheric teleconnections and greatly intensified haze pollution in NC. The eastern Atlantic/western Russia
40 (EA/WR), western Pacific (WP) and Eurasia (EU) patterns served as effective atmospheric bridges linking distant and
41 preceding external factors to the anomalous anticyclonic circulations over Northeast Asia (Yin and Wang, 2017; Yin et al.,
42 2017). With enhanced anticyclonic anomalies, the haze pollution in NC was significantly aggravated by poor ventilation
43 conditions and high moisture.

44 The long-term trend of haze pollution has always been attributed to increasing human activities directly related to aerosol
45 emissions (Yang et al., 2016; Li et al., 2018). It is true that emissions are important in the formation of haze, but their role
46 varies from region to region (Mao et al., 2019). The trend of haze days in Yangtze River Delta and Pearl River Delta was
47 closely related to the trend of particle emissions (Fig. S1b, c), while a weak correlation existed in Fenwei Plain (Fig. S1d). A
48 surprising phenomenon can be seen in NC: the number of winter haze days and particle emissions showed similar trends before
49 early 1990s, but afterward, their close relationship disappeared (Fig. S1a). Many recent studies also showed that the long-term
50 trend in the haze problem has likely been driven by global warming (Horton et al, 2014; Cai et al., 2017). Weakening surface
51 winds have been reported over land in the last few decades while the global surface air temperature (SAT) has warmed
52 significantly (McVicar et al., 2012). In addition, enhanced vertical stability, which favors the accumulation of pollutants, has
53 been observed with global warming (Liu et al., 2013). However, none of the above studies focused on the change in the haze
54 trend. Over the past few decades, the global and Northern Hemispheric SAT averages generally displayed a continuous
55 warming trend, which was not exactly similar to the trend of haze days in NC (Fig. S2). It follows that haze pollution, especially
56 the change in its trend, is regulated by multiple drivers and that the long-term impacts of external forcing factors, which
57 efficiently modulate the interannual and decadal variations in haze, deserve further investigation.

58 **2 Datasets and Methods**

59 **2.1 Data description**

60 Monthly mean meteorological data from 1979 to 2018 were obtained from NCEP/NCAR reanalysis datasets (2.5 °×2.5 °),
61 including the geopotential height at 500 hPa (H500), vertical wind from the surface to 150 hPa, surface air temperatures (SAT),
62 wind speed, and special humidity at the surface (Kalnay et al., 1996). The boundary layer height (BLH, 1 °×1 °) values were
63 from Interim reanalysis data (ERA-Interim) obtained from the European Centre for Medium-Range Weather Forecasts
64 (ECMWF) (Dee et al., 2011). The number of haze days was calculated from the long-term meteorological data, mainly based
65 on observed visibility and relative humidity (Yin et al., 2017). The PM_{2.5} concentrations from 2009 to 2016 were acquired
66 from the US embassy, and those from 2014 to 2018 were from China National Environmental Monitoring Centre. Monthly
67 total emissions of BC, NH₃, NO_x, OC, SO₂, PM₁₀ and PM_{2.5} are obtained from the Peking University emission inventory. The
68 monthly mean extended reconstructed SST data (2 °×2 °) were obtained from the National Oceanic and Atmospheric
69 Administration (Smith et al., 2008). The monthly snow cover data were supported by the Rutgers University (Robinson et al.,
70 1993). And the monthly soil moisture data (0.5 °×0.5 °) were downloaded from NOAA's Climate Prediction Center (Huug et
71 al., 2003)

72 2.2 Geos-Chem description and experimental design

73 We used the GEOS-Chem model to simulate PM_{2.5} concentrations (<http://acmg.seas.harvard.edu/geos/>). The GEOS-
74 Chem model was driven by MERRA-2 assimilated meteorological data (Gelaro et al., 2017). The nested grid over Asia (11 °S–
75 55 °N, 60–150 °E) had a horizontal resolution of 0.5° latitude by 0.625° longitude and 47 vertical layers up to 0.01 hPa. The
76 GEOS-Chem model includes fully coupled O₃-NO_x-hydrocarbon and aerosol chemical mechanisms with more than 80 species
77 and 300 reactions (Bey et al., 2001; Park et al., 2004). The PM_{2.5} components simulated in GEOS-Chem include sulfate, nitrate,
78 ammonium, black carbon and primary organic carbon, mineral dust, secondary organic aerosols and sea salt. At present,
79 GEOS-Chem model has been widely used, Dang et al. (2019) showed that the simulated spatial patterns and daily variations
80 of winter PM_{2.5} based on this model agree well with the observations from 2013 to 2017, available years with measured PM_{2.5},
81 We selected the year of 2015, which has just begun to strengthen emission reduction, and 2017, which has launched the air
82 pollution prevention and management plan for “2+26” cities (Yin and Zhang, 2020), as two representative years to simulate
83 the actual PM_{2.5} concentrations, so as to evaluate the performance of the GEOS-Chem model. The simulation results are very
84 close to the observed data (Fig. S3) with high correlation coefficients reaching 0.88 and 0.85 in 2015 and 2017, indicating this
85 model could basically reflect the change of actual PM_{2.5} concentrations.

86 In this study, we designed two kinds of experiments. One was an experiment for simulating PM_{2.5}, and the other was a
87 composite using simulated data. The simulation had changing meteorological fields in winter from 1980 to 2018 and the fixed
88 emissions in 2010 representing a high emission level. The emissions data in 2010 were from MIX 2010 (Li et al., 2017). The
89 numerical experiment was performed to examine the variation of PM_{2.5} in the meteorological parameters during 1980–2018
90 under fixed-emission scenarios.

91 The composite was conducted to analyze the differences in the simulated HD_{NC} according to the years selected for the
92 external forcing factors. Using the simulated dataset with the fixed-emission scenario was capable of eliminating the impacts
93 of emissions and simply considering the effect of the four external forcing factors. The four (two) years with the largest (Favor
94 Years) and smallest (Unfavor Years) four external forcing indices (i.e., SST_P, -1 × SST_A, Snow_c and -1 × Soil_w) were selected,
95 and the differences in the simulated HD_{NC} under these four conditions in P1 (P2) were calculated. The simulated HD_{NC} in
96 Favor Years minus the simulated HD_{NC} in Unfavor Years was calculated to analyze the effect of these four forced factors.

97 2.3 Statistical methods

98 In this study, the statistical model of fitted HD_{NC} was built based on Multiple Linear Regression (MLR). This approach,
99 a model-driven method, was ultimately expressed as a linear combination of K predictors (x_i) that could generate the least
100 error of prediction \tilde{y} (Wilks, 2011). With coefficients β_i , intercept β_0 , and residual ε , the MLR formula can be written in
101 the following form: $\tilde{y} = \beta_0 + \sum \beta_i x_i + \varepsilon$.

102 The trends calculated in this study were obtained by linear regression after a 5-year running average. This method removed
103 the interannual variation and more prominent trend characteristics. Moreover, the stage trends were calculated according to
104 the inflection point, which passed the Mann-Kendall test.

105 3 Trend change of early winter haze

106 Throughout the winter in North China, the haze pollution in early winter is the most serious (Yin et al., 2019). The number
107 of haze days in early winter (December and January) in North China (HD_{NC}) reached a remarkable inflection point in 2010
108 (Fig. 1a), passing the Mann-Kendall Test. The trend of HD_{NC} was vastly different before and after 2010: slowly decreased
109 during 1991–2010 (P1) with a rate of 4.67 days/10 yr but rapidly increased after 2010 (P2, 2010–2018) with a rate of 25.43
110 days/10 yr, both of them passing 95% t test. Recent studies generally revealed that based on observations, the number of boreal
111 winter haze days across NC had a slightly decreasing trend after 1990 (Ding and Liu, 2014; He et al., 2019; Mao et al., 2019;
112 Shi et al., 2019), which is consistent with the decreasing trend presented by the dataset in our research. Excluding year 2010
113 did not affect the change in the trend of the two periods, with a decreased rate of 3.82 days/10 yr during 1991–2009, and an
114 increased rate of 20.76 days/10 yr during 2011–2018 (passing 95% t test). In addition, Dang and Liao (2019) confirmed the
115 varying trend of HD_{NC} via simulations of the global 3-D chemical transport (GEOS-Chem) model; using the well-simulated
116 frequency of serious haze days in winter, they also revealed the abovementioned changing trend of HD_{NC}, i.e., decreasing in
117 the early stage and increasing in the later stage. To further determine the reliability of the post-2010 upward trend of HD_{NC},
118 we used hourly PM_{2.5} concentrations observed at the US embassy in Beijing from 2009 to 2017 and ~~those~~ the PM_{2.5}
119 concentrations over North China monitored by China National Environmental Monitoring Centre from 2014 to 2018 to count
120 the number of days when the PM_{2.5} concentrations were >75 $\mu\text{g m}^{-3}$ and >100 $\mu\text{g m}^{-3}$ (Fig. 1a). These statistics also reflected

121 the rising trend after 2010, as well as the improved air quality in 2017 and a rebound in pollution in 2018. Although there was
122 a certain gap between HD_{NC} (basing on visibility and humidity) and these statistics, the two datasets revealed the same
123 variations after 2010, and the statistics confirmed the robustness of the observed HD_{NC}.

124 The above analysis substantiated the rapid aggravation of haze pollution in early winter after 2010. With regard to the
125 increase in air pollution, there is no doubt that anthropogenic emissions were the fundamental cause of this long-term variation.
126 Before the mid-2000s, the particle emissions throughout NC sustained stable growth but gradually began to decline afterward,
127 which is inconsistent with the trend of HD_{NC} or even contrary in some subperiods. The previous decreasing trend of HD_{NC} hid
128 the effects of the increased pollutant emissions; thus, people ignored the pollution problem and failed to control it in time. As
129 a consequence, the subsequent rise in HD_{NC} was extremely rapid and seriously harmed the biological environment and human
130 health. The stark discrepancy between the trends of pollutant emissions and HD_{NC} strongly indicate that anthropogenic
131 emissions were not the only factor leading to a sharp deterioration in air quality after 2010 (Wei et al., 2017; Wang 2018).
132 Therefore, an important question must be asked: in addition to human activities, what factors caused the rapidly increasing
133 trend of HD_{NC} after 2010?

134 As mentioned above, local meteorological factors could modulate the capacity to disperse and the formation of haze
135 particles, which have critical influences on the occurrence of severe haze pollution. To reveal the impacts of meteorological
136 conditions on the changing trend of HD_{NC}, the area-averaged linear trends of these meteorological factors in NC during P1 and
137 P2 were calculated, all of which exceeded the 95% confidence level (Fig. 2). In P1, the area-averaged linear trends of the
138 boundary layer height (BLH), wind speed and omega all showed significant positive trends, while specific humidity showed a
139 significant negative trend in NC; these conditions favored a superior air quality (Niu et al., 2010; Ding and Liu, 2014; Yin et
140 al., 2017; Shi et al., 2019; Zhong et al., 2019). However, the trends of these four meteorological factors completely reversed
141 in P2. Reductions in the BLH and wind speed, the enhancement of moisture, and an anomalous descending motion resisted
142 the vertical and horizontal dispersions of particles and helped more pollutants gather in relatively narrow spaces. These four
143 meteorological factors expressed an evident influence on the change trend of HD_{NC} and showed reversed trends between P1
144 and P2, similar to HD_{NC}. Furthermore, the magnitudes of the change rates of these factors were stronger in P2 than in P1 (Fig.
145 2), and HD_{NC} displayed this feature as well. The GEOS-Chem simulations with changing emissions and fixed meteorological
146 conditions failed to reproduce the change trend of haze (Dang and Liao, 2019), but with varying meteorology and fixed
147 emissions could recognize the interannual variation of haze days. We designed an experiment driven by changing
148 meteorological conditions in winter from 1980 to 2018 and fixed emissions at the relatively high 2010 level. According to the
149 technical regulation on the ambient air quality index (Ministry of Ecology and Environment of the People's Republic of China,
150 2012), a haze day was defined as a day with daily mean PM_{2.5} concentration exceeding 75 $\mu\text{g m}^{-3}$. The simulations of the
151 frequency of haze days in NC by GEOS-Chem reproduced the trend reversal of haze pollution (Fig. 1b). The simulation results

152 were highly correlated with HD_{NC} and showed the feature that the trend in P2 was stronger than that in P1, indicating that
153 meteorological conditions drove the trend change of haze pollution.

154 4 Climate variability drove the trend reversal

155 According to many previous studies, the variabilities of the Pacific SST, Atlantic SST, Eurasian snow cover and Asian
156 soil moisture played key roles in the interannual variations in haze pollution in NC (Xiao et al., 2015; Yin and Wang, 2016a,
157 b; Zou et al., 2017), and the associated physical mechanisms were evidently revealed. Thus, the following question is raised
158 here: did these four factors drive the trend reversal of HD_{NC} , and if so, how?

159 As shown in Figure S43a, the preceding autumn SST in the Pacific, associated with the detrended HD_{NC} , presented a
160 Pacific Decadal Oscillation (PDO)-like “triple pattern” with two significant positive regions and one nonsignificant negative
161 region (Yin and Wang, 2016a; Zhao et al., 2016). In the following research, the SST anomalies in the two positively correlated
162 regions located in the Gulf of Alaska (40–60 °N, 125–165 °W) and the central eastern Pacific (5–25°N, 160 °E–110 °W) were
163 used to represent the effects originating from the North Pacific. The area-averaged September–November SST of these two
164 regions was calculated as the SST_P index, and the correlation coefficients with HD_{NC} were 0.59 and 0.67 before and after
165 removing the linear trend during 1979–2018, respectively; both correlation coefficients were above the 99% confidence level.
166 The responses of the atmosphere to these positive SST_P anomalies were the positive phase of the EA/WR pattern and the
167 enhanced anomalous anticyclone center over NC (Yin et al., 2017; Fig. S54). Modulating by such large-scale atmospheric
168 anomalies, increased moisture, anomalous upward motion and reduced BLH and wind speed (Fig. S54) created a favorable
169 environment for the accumulation of fine particles (Niu et al., 2010; Ding and Liu, 2014; Shi et al., 2019; Zhong et al., 2019).
170 A numerical experiment based on the Community Atmosphere Model version 5 (CAM5) effectively reproduced the observed
171 enhanced anticyclonic anomalies over Mongolia and North China in response to positive PDO forcing, which resulted in an
172 increase in the number of wintertime haze days over central eastern China (Zhao et al., 2016). The trend changes of the North
173 Pacific SST were examined in P1 and P2. Consistent with the changing trend of HD_{NC} , reversed trends were also found in the
174 North Pacific, i.e., a significant negative trend during P1 and a positive trend during P2 over the two Pacific areas (Fig. 3a, b).
175 These similar trend changes suggest that the North Pacific SST might have been a major driver of the abrupt change in HD_{NC} .
176 It is clear that SST_P underwent a significant trend change around 2010 (Fig. 4a). Thus, the persistent decline in SST_P during P1
177 (at a significant rate of $-0.2\text{ °C}/10\text{ yr}$, passing 95% t test; Table 1) contributed to the slowly decreasing trend of HD_{NC} (Fig.
178 4a) via the modulations of SST_P on the atmospheric circulation (Fig. S54). During P2, the larger increase in SST_P at a rate of
179 $2.0\text{ °C}/10\text{ yr}$ (passing 95% t test) dramatically drove the rapid increase in HD_{NC} .

180 Besides the triple pattern in the Pacific, two areas exhibiting significant negative correlations with HD_{NC} were examined
181 in the Atlantic (Shi et al., 2015; Shi et al., 2015): one located over southern Greenland (50–68 °N, 18–60 °W) and another

182 located over the equatorial Atlantic (0–15 °N, 30–60 °W; Fig. S43a). The area-averaged September–November SST of the two
183 negatively correlated regions in Atlantic was defined as the SST_A index, whose correlation coefficients with HD_{NC} were –0.55
184 and –0.64 from 1979 to 2018 before and after detrending, respectively (above the 99% confidence level). The response of
185 atmospheric circulation to these negative SST_A anomalies culminated in a positive EA/WR pattern, and the stimulated easterly
186 weakened the intensity of East Asian jet stream (EAJS) in the high troposphere (Fig. S65). Influenced by the colder SST_A,
187 there was a very obvious abnormal upward movement above the boundary layer, reducing both the BLH and the surface wind
188 speed; thus, pollutants were prone to gather, causing haze pollution (Niu et al., 2010; Wu et al., 2017; Shi et al., 2019). With
189 a linear barotropic model, Chen confirmed the important role of subtropical northeastern Atlantic SST anomalies in
190 contributing to the anomalous anticyclone over Northeast Asia and anomalous southerly winds over NC, which enhanced the
191 accumulation of pollutants (Chen et al., 2019). The spatial linear trend in the SST of both Atlantic areas changed from positive
192 in P1 to negative in P2, which was completely contrary to the trend of HD_{NC} (Fig. 3a, b). The SST_A reached a inflection point
193 in 2010 (Fig. 4b) and contributed to the falling of HD_{NC} during P1 (change rate of SST_A = 0.55 °C/10 yr, passing 95% t test)
194 and the rising of HD_{NC} during P2 (change rate of SST_A = –0.52 °C/10 yr, passing 95% t test).

195 The effect of Eurasian snow cover on the number of December haze days in NC intensified after the mid-1990s (Yin and
196 Wang, 2018). The roles of extensive boreal Eurasian snow cover were also revealed by numerical experiments via the
197 Community Earth System Model (CESM): positive snow cover anomalies enhanced the regional circulation mode of poor
198 ventilation in NC and provided conducive conditions for extreme haze (Zou et al., 2017). The correlation between the October–
199 November snow cover and HD_{NC} was significantly positive in eastern Europe and western Siberia (46–62 °N, 40–85 °E, Fig.
200 S43b), where the spatial linear trend of snow cover was consistent with that of HD_{NC}. A significant negative trend in P1 and a
201 positive trend in P2 were discovered (Fig. 3c, d). The area-averaged October–November snow cover over eastern Europe and
202 western Siberia was defined as the Snowc index, and its correlation coefficients with HD_{NC} were 0.43 and 0.54 from 1979 to
203 2018 before and after detrending, respectively (above the 99% confidence level). The features of the weakened EAJS and
204 significant anomalous anticyclone could be found clearly in the induced atmospheric anomalies associated with the positive
205 Snowc anomalies (Fig. S76). The related abnormal upward motion restricted the momentum to the surface. In addition, the
206 corresponding lower BLH and weaker surface wind speed also reduced the dispersion capacity, resulting in the generation of
207 more haze pollution (Fig. S76). The Snowc index fell slowly until 2010 (with a rate of –1.8%/10 yr, passing 95% t test) and
208 then rose rapidly (with a rate of 28.3%/10 yr, passing 95% t test) and experienced a large trend reversal in 2010, in accordance
209 with the behavior of HD_{NC} (Fig. 4c). Therefore, relying on the revealed physical mechanisms, the strengthened relationship
210 between Snowc and HD_{NC} and the tremendous increase in Snowc during P2 substantially triggered the rapid enhancement of
211 haze pollution in NC.

212 In addition to snow cover, soil moisture was another important factor affecting HD_{NC} (Yin and Wang, 2016b). The
213 September-November soil moisture and HD_{NC} were negatively correlated in central Siberia (54–70°N, 80–130°E; Fig. S43c).
214 The area-averaged September-November soil moisture over central Siberia was denoted as the Soilw index, whose correlation
215 coefficients with HD_{NC} were –0.57 and –0.60 from 1979 to 2018 before and after detrending, respectively (above the 99%
216 confidence level). Negative Soilw anomalies could induce a positive phase of EA/WR, and the associated anticyclonic
217 circulations occurred more frequently and more strongly (Fig. S87). Correspondingly, the local vertical and horizontal
218 dispersion conditions were limited. With increasing moisture, pollutants can more easily accumulate in a confined area. The
219 spatial linear trend of soil moisture also shifted from increasing to decreasing in 2010, opposite to the trend of HD_{NC} (Fig. 3e,
220 f). The change rate of Soilw was 38.8 mm/10 yr passing 95% t test (opposite that of HD_{NC}) during P1, and the rate of change
221 became more intense (–51.8 mm/10 yr, passing 95% t test) during P2, physically driving a similar large change in HD_{NC} (Fig.
222 4d).

223 The varying trends of these four preceding external factors jointly drove the trend reversal of HD_{NC} based on their physical
224 relationships with the haze pollution in North China. To exclude the impacts of the stage trends of these variables on the
225 physical links between the climate drivers and HD_{NC}, the correlations between these factors and HD_{NC} were explored during
226 the decreasing stage (i.e., 1979–2010) and increasing stage (2010–2018), and all of these correlations were significant (Table
227 1). Thus, the physical relationships between HD_{NC} and these four factors were long-standing and did not disappear as the trend
228 changed. These four external factors had completely opposite trends in P1 and P2. Excluding SST_A, the amplitudes of the
229 change trends of the other three indices in P2 were obviously stronger than those in P1 and were identical to those of HD_{NC}
230 (Table 1). In our study, we composited the simulations based on the GEOS-Chem model to determine the impact on haze
231 pollution of each factor under the fixed-emissions level. The years in the top 20% and the bottom 20% of the four indices (i.e.,
232 SST_P, –1×SST_A, Snowc and –1×Soilw) in P1 and P2 were selected, which could remove the effects of different trends. The
233 composite differences for the four external forcing factors were significant in the selected regions and passed the Student's t
234 test (Fig. S98). The responses of simulated HD_{NC} to the original (detrended) sequences of SST_P, SST_A, Snowc and Soilw were
235 all positive, which are consistent with the observational results (Fig. 5). Specifically, for the four original (detrended) drivers,
236 the resulting differences in simulated HD_{NC} were 3.94 (5.28), 5.97 (5.07), 1.86 (1.86) and 6.49 (6.49) days in P1 and 4.46
237 (4.46), 4.26 (4.26), 7.54 (7.54) and 7.35 (7.35) days in P2 (Fig. 5). These differences were distinct and further confirmed that
238 each factor played a role in the occurrence of haze pollution in NC.

239 These four indices were employed to linearly fit HD_{NC} based on a multiple linear regression (MLR) model (Wilks, 2011).
240 As shown in Figure 4e, the correlation coefficient between the fitted and observed HD_{NC} was 0.82. After a five-year running
241 average, the correlation coefficient reached 0.92. This model showed good ability to fit the inflection point in 2010 and
242 highlighted the trend changes. Such a good fitting effect indicates that changes in the four external forcing factors could well

243 have influenced the variation in HD_{NC} . By exciting stronger responses in the atmosphere, such as the positive EA/WR phase
244 and the strengthened anomalous anticyclone over NC, the abovementioned climate drivers created stable and stagnant
245 environments in which the haze pollution in NC could rapidly exacerbate after 2010 (Table 1). Among the four indices, the
246 correlation coefficients between SST_P and $Snowc$ (Pair 1) and between SST_A and $Soilw$ (Pair 2) were high, while the rest were
247 insignificant. The variance inflation factors of the four factors in the MLR model were less than 2, showing that the collinearity
248 among them was weak. When selecting one factor from both Pair 1 and Pair 2 to refit HD_{NC} , the correlation coefficient between
249 the fitted and observed HD_{NC} and the trends of the fitted HD_{NC} in P2 worsened (Fig. S109). Therefore, these four external
250 factors were all indispensable to achieve a better fitting effect. The intercorrelated climate factors of Pair 1 and Pair 2
251 contributed 27.8% and 84.6%, respectively, to the trends of HD_{NC} in P1 and 54.8% and 20.4% to the trends in P2. Thus, the
252 joint effect of SST_A and $Soilw$ played a more important role in the decreasing trend of HD_{NC} in P1; however, the impacts of
253 SST_P and $Snowc$ were more than twice those of SST_A and $Soilw$ in P2. More importantly, the fitted curve revealed a decreasing
254 trend of HD_{NC} (-5.24 days/10 yr, passing 95% t test) that was larger than observed (-4.67 days/10 yr) during P1. Many studies
255 have noted that human activities have led to persistently increasing trends of HD_{NC} (Yang et al., 2016; Li et al., 2018). The
256 combination of the exorbitant decreased trend indicated by climate conditions and the long-term trend from anthropogenic
257 emissions resulted in a realistic slow decline (Table 2). This proportion of the trend explained by climate drivers (72.3%)
258 decreased in P2 because the increasing trend driven by the climate divers and emissions jointly led to a rapid increase in HD_{NC} .

259 5 Conclusions and discussions

260 Haze events in early winter in North China exhibited rapid growth after 2010, which was completely different from the
261 slow decline observed before 2010, showing a trend reversal in the year 2010 (Fig. 1). The trend changes of associated
262 meteorological conditions exhibited identical responses. After 2010, the lower BLH, weakened wind speed, sufficient moisture
263 and anomalous ascending motion (all with larger tendencies than before 2010) limited the horizontal and vertical dispersion
264 conditions and thus enhanced the occurrence of early winter haze pollution (Fig. 2). However, before 2010, the climate
265 conditions showed the opposite characteristics and could create an environment with adequate ventilation for the dissipation
266 of particles.

267 In this study, the external forcing factors that caused-closely related to the significant growth of HD_{NC} after 2010 and the
268 associated physical mechanisms were investigated. These factors could stimulate and strengthen-might strongly linked to the
269 anomalous anticyclone over NC via exciting the EA/WR teleconnection pattern, thus regulating the meteorological conditions,
270 weakening the dispersion conditions and facilitating the accumulation of haze pollutants. The four climate drivers physically
271 related to HD_{NC} showed exactly opposite trend changes with an inflection point in 2010, which agrees with the behavior of
272 HD_{NC} (Fig. 4). The factors of Pair 1 (SST_A and $Soilw$) and Pair 2 (SST_P and $Snowc$) had joint effects and played more important

273 roles in the increasing trend of HD_{NC} in P2 and the decreasing trend of HD_{NC} in P1, respectively (Table 2). The fitting result
274 of the four factors with the trend of HD_{NC} showed a strongly decreasing trend in P1 and a weakly increasing trend in P2.
275 Together with increasing emissions, these factors jointly led to a relatively slow decreasing trend of HD_{NC} before 2010 and
276 rapid growth afterward. Therefore, both the decreasing trend in P1 and the increasing trend in P2 were caused by a combination
277 of climate drivers and emissions.

278 Note that a number of factors contribute to the uncertainties in our results. Although a high emission scenario was used
279 to simulate the number of haze days and emphasized the influence of meteorology, no complete and varied emission inventories
280 were used to drive the GEOS-Chem model to make a comparison, which caused certain uncertainty. Furthermore, when
281 assessing the contribution percentages of the external forcing factors, the coupling effect between climate variability and
282 anthropogenic emissions was not considered, therefore the contribution rate of climate conditions might be overestimated.

283 For the long-term trend of haze, human activities are the recognized and fundamental driver (Li et al., 2018; Yang et al
284 2016). Anthropogenic emissions have exceeded a high level since the 1990s, providing a sufficient foundation for the
285 generation of severe haze pollution (Fig. 1). However, the effects of climate variability delayed warnings before 2010. Together
286 with the local meteorological conditions, the trends of the climate drivers reversed in 2010, initiating a dramatically increase
287 in HD_{NC} after 2010, which quickened the worsening of haze pollution in NC (Fig. 5; Table 1). The superimposed effect of
288 high-level human emissions with strengthened climate anomalies loudly sounded the alarms through the extremely rapid rise
289 of haze pollution.

290 *Data availability.* The monthly mean meteorological data are obtained from NCEP/NCAR reanalysis datasets
291 (<https://www.esrl.noaa.gov/psd/data/gridded/data.ncep.reanalysis.html>). The boundary layer height data are available from the
292 Interim reanalysis dataset (<http://www.ecmwf.int/en/research/climate-reanalysis/era-interim>). The number of haze days can be
293 obtained from the authors. The PM_{2.5} concentrations from 2009 to 2016 can be downloaded from the US embassy
294 (<http://www.stateair.net/web/historical/1/1.html>), and those from 2014 to 2018 can be downloaded from China National
295 Environmental Monitoring Centre (<http://beijingair.sinaapp.com/>). The monthly total emissions of BC, NH₃, NO_x, OC, SO₂,
296 PM₁₀ and PM_{2.5} are obtained from the Peking University emission inventory (<http://inventory.pku.edu.cn/>). SST data are
297 downloaded from <http://www.esrl.noaa.gov/psd/data/gridded/data.noaa.ersst.v4.html>. Soil moisture data are obtained from
298 <https://www.esrl.noaa.gov/psd/data/gridded/data.cpcsoil.html>. Snow cover data can be downloaded from Rutgers University:
299 <http://climate.rutgers.edu/snowcover/>. The emissions of 2010 can be downloaded from
300 <http://geoschemdata.computecanada.ca/ExtData/HEMCO/MIX>.

301 **Acknowledgements**

302 This work was supported by the National Key Research and Development Plan (2016YFA0600703), National Natural Science
303 Foundation of China (41705058, 41991283 and 91744311), and the funding of Jiangsu innovation & entrepreneurship team.

304 **Author contributions**

305 Wang H. J. and Yin Z. C. designed the research. Yin Z. C. and Zhang Y. J. performed research. Zhang Y. J. prepared the
306 manuscript with contributions from all co-authors.

307 **Competing interests**

308 The authors declare no conflict of interest.

309 **References**

310 Bey, I., Jacob, D. J., Yantosca, R. M., Logan, J. A., Field, B. D., Fiore, A. M., Li, Q. B., Liu, H. G. Y., Mickley, L. J., and
311 Schultz, M. G.: Global modeling of tropospheric chemistry with assimilated meteorology: Model description and evaluation,
312 *J. Geophys. Res.-Atmos.*, 106, 23073–23095, <https://doi.org/10.1029/2001jd000807>, 2001.

313 Cai, W., Li, K., Liao, H., Wang, H., and Wu, L.: Weather conditions conducive to Beijing severe haze more frequent under
314 climate change, *Nat Clim Change*, 7, 257–262, 2017.

315 Chen, S., Guo, J., Song, L., Li, J., Liu, L., and Cohen, J.: Inter-annual variation of the spring haze pollution over the North
316 China Plain: Roles of atmospheric circulation and sea surface temperature, *Int. J. Climatol.*, 39, 783–798, 2019.

317 Cohen, A., Brauer, M., Burnett, R., Anderson, H., Frostad, J., Estep, K., Balakrishnan, K., Brunekreef, B., Dandona, L.,
318 Dandona, R., Feigin, V., Freedman, G., Hubbell, B., Jobling, A., Kan, H., Knibbs, L., Liu, Y., Martin, R., Morawska, L., Pope,
319 C., Shin, H., Straif, K., Shaddick, G., Thomas, M., Dingenen, R., Donkelaar, A., Vos, T., Murray, C., and Forouzanfar, M.:
320 Estimates and 25-year trends of the global burden of disease attributable to ambient air pollution: An analysis of data from the
321 Global Burden of Diseases Study 2015, *Lancet*, 389, 1907–1918, 2017.

322 Dang, R. and Liao, H.: Severe winter haze days in the Beijing-Tianjin-Hebei region from 1985 to 2017 and the roles of
323 anthropogenic emissions and meteorology, *Atmos. Chem. Phys.*, 19, 10801–10816, 2019.

324 Dee, D. P., Uppala, S. M., Simmons, A. J., Berrisford, P., Poli, P., Kobayashi, S., Andrae, U., Balmaseda, M. A., Balsamo,
325 G., Bauer, P., Bechtold, P., and Beljaars, A. C. M.: The ERA Interim reanalysis: configuration and performance of the data
326 assimilation system, *Q. J. Roy. Meteor. Soc.*, 137, 553–597, <https://doi.org/10.1002/qj.828>, 2011.

327 Ding, D. and Liu, Y.: Analysis of long-term variations of fog and haze in China in recent 50 years and their relations with
328 atmospheric humidity, *Sci. China Ser. D.*, 57, 36–46, 2014.

329 Gelaro, R., McCarty, W., Suarez, M. J., Todling, R., Molod, A., Takacs, L., Randles, C. A., Darmenov, A., Bosilovich, M. G.,
330 Reichle, R., Wargan, K., Coy, L., Cullather, R., Draper, C., Akella, S., Buchard, V., Conaty, A., da Silva, A. M., Gu, W., Kim,
331 G. K., Koster, R., Lucchesi, R., Merkova, D., Nielsen, J. E., Partyka, G., Pawson, S., Putman, W., Rienecker, M., Schubert, S. D.,
332 Sienkiewicz, M., and Zhao, B.: The Modern-Era Retrospective Analysis for Research and Applications, Version 2 (MERRA2),
333 *J. Climate*, 30, 5419–5454, <https://doi.org/10.1175/jcli-d-160758.1>, 2017.

334 He, C., Liu, R., Wang, X., Liu, S., Zhou, T., and Liao, W.: How does El Niño-Southern Oscillation modulate the interannual
335 variability of winter haze days over eastern China? *Sci. Total Environ.*, 651, 1892–1902, 2019.

336 Huug, D., Huang, J., and Fan, Y.: Performance and analysis of the constructed analogue method applied to US soil moisture
337 applied over 1981–2001, *J. Geophys. Res.*, 108, 1–16, 2003.

338 Horton, D., Skinner, C., Singh, D., Diffenbaugh, N.: Occurrence and persistence of future atmospheric stagnation events, *Nat.*
339 *Clim. Change*, 4, 698–703, 2014. Kalnay, E., Kanamitsu, M., Kistler, R., Collins, W., Deaven, D., Gandin, L., Iredell, M., Saha,
340 S., White, G., Woollen, J., Zhu, Y., Leetmaa, A., Reynolds, R., Chelliah, M., Ebisuzaki, W., Higgins, W., Janowiak, J., Mo, K.
341 C., Ropelewski, C., Wang, J., Jenne, R., and Joseph, D.: The NCEP/NCAR 40-year reanalysis project, *B. Am. Meteorol. Soc.*,
342 77, 437–471, [https://doi.org/10.1175/1520-0477\(1996\)077<0437:TNYRP>2.0.CO;2](https://doi.org/10.1175/1520-0477(1996)077<0437:TNYRP>2.0.CO;2), 1996.

343 Li, K., Liao, H., Cai, W., and Yang, Y.: Attribution of anthropogenic influence on atmospheric patterns conducive to recent
344 most severe haze over eastern China, *Geophys. Res. Lett.*, 45, 2072–2081, 2018.

345 Li, M., Zhang, Q., Kurokawa, J.-I., Woo, J.-H., He, K., Lu, Z., Ohara, T., Song, Y., Streets, D. G., Carmichael, G. R., Cheng,
346 Y., Hong, C., Huo, H., Jiang, X., Kang, S., Liu, F., Su, H., and Zheng, B.: MIX: a mosaic Asian anthropogenic emission
347 inventory under the international collaboration framework of the MICS-Asia and HTAP, *Atmos. Chem. Phys.*, 17, 935–963,
348 <https://doi.org/10.5194/acp-17-935-2017>, 2017.

349 Liu, J., Wang, B., Cane, M., Yim, S., and Lee, J.: Divergent global precipitation changes induced by natural versus
350 anthropogenic forcing, *Nature*, 493, 656–659, 2013.

351 Lu, X., Lin, C., Li, W., Chen, Y., Huang, Y., Fung, J., and Lau, A.: Analysis of the adverse health effects of PM_{2.5} from 2001
352 to 2017 in China and the role of urbanization in aggravating the health burden, *Sci. Total Environ.*, 652, 683–695, 2019.

353 Mao, L., Liu, R., Liao, W., Wang, X., Shao, M., Liu, S., and Zhang, Y.: An observation-based perspective of winter haze days
354 in four major polluted regions of China, *Natl. Sci. Rev.*, 6, 515–523, 2019.

355 Mcvicar, T., Roderick, M., Donohue, R., Li, L., Niel, T., Thomas, A., Grieser, J., Jhajharia, D., Himri, Y., Mahowald, N.,
356 Mescherskaya, A., Kruger, A., Rehman, S., Dinpashoh, Y.: Global review and synthesis of trends in observed terrestrial near-
357 surface wind speeds: Implications for evaporation, *J Hydrol.*, 416, 182–205, 2012.

358 Ministry of Ecology and Environment of the People’s Republic of China: Ambient air quality standards, China Environmental
359 Science Press, Beijing, 2012.

360 Niu, F., Li, Z., Li, C., Lee, K., and Wang, M.: Increase of wintertime fog in China: Potential impacts of weakening of the
361 Eastern Asian monsoon circulation and increasing aerosol loading, *J. Geophys. Res.*, 115, D7, 2010.

362 Park, R. J., Jacob, D. J., Field, B. D., Yantosca, R. M., and Chin, M.: Natural and transboundary pollution influences on sulfate-
363 nitrate-ammonium aerosols in the United States: Implications for policy, *J. Geophys. Res.-Atmos.*, 109, D15204,
364 <https://doi.org/10.1029/2003jd004473>, 2004.

365 Robinson, D. A., Dewey, K. F., and Heim Jr., R.: Global snow cover monitoring: an update, *B. Am. Meteorol. Soc.*, 74, 1689–
366 1696, 1993.

367 Shi, Y., Hu, F., Lü, R., and He, Y.: Characteristics of urban boundary layer in heavy haze process based on Beijing 325m
368 tower data, *Atmos. Oceanic Sci. Lett.*, 12, 41–49, 2019.

369 Shi, X., Sun, J., Sun, Y., Bi, W., Zhou, X., and Yi, L.: The impact of the autumn Atlantic sea surface temperature three-pole
370 structure on winter atmospheric circulation, *Acta. Oceanol. Sin.*, 37, 33–40, 2015.

371 Shi, P., Zhang, G., Kong, F., Chen, D., Azorin-Molina, C., and Guijarro, J.: Variability of winter haze over the Beijing-Tianjin-
372 Hebei region tied to wind speed in the lower troposphere and particulate sources, *Atmos. Res.*, 215, 1–1, 2019.

373 Smith, T., Reynolds, R., Peterson, T., and Lawrimore, J.: Improvements to NOAA’s historical merged land–ocean surface
374 temperature analysis (1880–2006), *J. Climate*, 21, 2283–2296, 2008.

375 Xiao, D., Li, Y., Fan, S., Zhang, R., Sun, J., and Wang, Y.: Plausible influence of Atlantic Ocean SST anomalies on winter
376 haze in China, *Theor. Appl. Climatol.*, 122, 249–257, 2015.

377 Yang, Y., Liao, H., and Lou, S.: Increase in winter haze over eastern China in recent decades: Roles of variations in
378 meteorological parameters and anthropogenic emissions, *J. Geophys. Res. Atmos.*, 121, 13050–13065, 2016.

379 Yin, Z., Wang, H., and Guo, W.: Climatic change features of fog and haze in winter over North China and Huang-Huai Area,
380 *Sci. China Earth Sci.*, 58, 1370–1376, 2015.

381 Yin, Z. and Wang, H.: The relationship between the subtropical Western Pacific SST and haze over North-Central North China
382 Plain, *Int. J. Climatol.*, 36, 3479–3491, 2016a.

383 Yin, Z. and Wang, H.: Seasonal prediction of winter haze days in the north central North China Plain, *Atmos. Chem. Phys.*,
384 16, 14843–14852, 2016b.

385 Yin, Z., and Wang, H.: Role of atmospheric circulations in haze pollution in December 2016, *Atmos. Chem. Phys.*, 17, 11673–
386 11681, 2017.

387 Yin, Z. and Wang, H.: The strengthening relationship between Eurasian snow cover and December haze days in central North
388 China after the mid-1990s, *Atmos. Chem. Phys.*, 18, 4753–4763, 2018.

389 Yin, Z., Li, Y., and Wang, H.: Response of Early Winter Haze Days in the North China Plain to Autumn Beaufort Sea Ice.
390 *Atmos. Chem. Phys.*, 19, 1439–1453, 2019.

391 Yin, Z., Wang, H., and Chen, H.: Understanding severe winter haze events in the North China Plain in 2014: Roles of climate
392 anomalies, *Atmos. Chem. Phys.*, 17, 1641–1651, 2017.

393 Wang, H.: On assessing haze attribution and control measures in China, *Atmos. Oceanic Sci. Lett.*, 11, 120–122, 2018.

394 Wang, H. and Chen, H.: Understanding the recent trend of haze pollution in eastern China: roles of climate change, *Atmos.*
395 *Chem. Phys.*, 16, 4205–4211, 2016.

396 Wei, Y., Li, J., Wang, Z., Chem, H., Wu, Q., Li, J., Wang, Y., and Wang, W.: Trends of surface PM_{2.5} over Beijing–Tianjin–
397 Hebei in 2013–2015 and their causes: emission controls vs. meteorological conditions, *Atmos. Oceanic Sci. Lett.*, 10, 276–
398 283, 2017.

399 Wilks, D.: *Statistical methods in the atmospheric sciences*, Academic press, Oxford, 2011.

400 Wu, P., Ding, Y., and Liu, Y.: Atmospheric circulation and dynamic mechanism for persistent haze events in the Beijing–
401 Tianjin–Hebei region, *Adv. Atmos. Sci.*, 34, 429–440, 2017.

402 Zhang, Q. and Crooks, R.: *Toward an environmentally sustainable future: Country environmental analysis of the People’s*
403 *Republic of China*, China Financial and Economic Publishing House, Beijing, 2012.

404 Zhao, S., Li, J., and Sun, C.: Decadal variability in the occurrence of wintertime haze in central eastern China tied to the Pacific
405 Decadal Oscillation, *Sci. Rep.*, 6, 27424, 2016.

406 Zhong, W., Yin, Z., and Wang, H.: The Relationship between the Anticyclonic Anomalies in Northeast Asia and Severe Haze
407 in the Beijing-Tianjin-Hebei Region, *Atmos. Chem. Phys.*, 19, 5941–5957, 2019.

408 Zou, Y., Wang, Y., Zhang, Y., and Koo, J.: Arctic sea ice, Eurasia snow, and extreme winter haze in China, *Sci. Adv.*, 3,
409 e1602751, 2017.

410 **Table and Figure legends**

411 Table 1. Correlation coefficients (CCs) between HD_{NC} and the SST_P, SST_A, Snow_C and Soil_w indices after detrending and the
412 trends of the SST_P, SST_A, Snow_C and Soil_w indices for the periods 1991–2010 and 2010–2018. CC₁, CC₂, and CC₃ represent
413 the correlation coefficients from 1979 to 2018, 1979 to 2010 and 2010 to 2018, respectively. “***” indicates that the CC was
414 above the 99% confidence level, “**” indicates that the CC was above the 95% confidence level, and “*” indicates that the
415 CC was above the 90% confidence level.

416 Table 2. The contribution rate of fitted HD_{NC} and each external forcing factor to the trend of HD_{NC} in P1 and P2, respectively.

417 Figure 1. (a) Variations in the December-January emissions (unit: Tg) of black carbon (BC), ammonia (NH₃), nitrogen oxide
418 (NO_x), organic carbon (OC), sulfur dioxide (SO₂), PM₁₀ and PM_{2.5} over North China from 1979 to 2013 and the variation in
419 HD_{NC} from 1979 to 2018 (black solid line). ~~The red dashed line represents the total emissions of the seven pollutants.~~ The blue
420 and green solid (dashed) lines indicate the number of days when the hourly PM_{2.5} concentrations in a day exceeded 75 μg m⁻³

421 and $100 \mu\text{g m}^{-3}$, respectively, from 2009 to 2016 (2014 to 2018) using [Beijing \(North China\)](#) observed data from the US
422 embassy (China National Environmental Monitoring Centre). (b) Temporal evolutions of HD_{NC} (in black), simulated haze
423 days (unit: days; red) in NC. The dashed lines denote linear regressions for 1991–2010 (P1) and 2010–2018 (P2). [The black](#)
424 [and red](#) Trend 1 and Trend 2 represent the linear trends of the [observed and simulated haze days](#) in P1 and P2, respectively.

425 Figure 2. Area-averaged linear trends of the BLH (unit: m/yr), specific humidity (unit: $\%/10 \text{ yr}$), surface wind speed (unit: m
426 $\text{s}^{-1}/10^2 \text{ yr}$) and omega (unit: $\text{pascal s}^{-1}/10^3 \text{ yr}$) over NC in early winter for the periods 1991–2010 (P1) and 2010–2018 (P2).
427 All datasets were 5-year running averages before calculating the trends.

428 Figure 3. Linear trends of the Pacific and Atlantic SST (unit: $^{\circ}\text{C/yr}$; a, b), Eurasian snow cover (unit: $\%/yr$; c, d), and central
429 Siberian soil moisture (unit: mm/yr ; e, f) for the periods 1991–2010 (P1) and 2010–2018 (P2). All datasets were 5-year running
430 averages before calculating the trends. The green boxes represent the regions where the four indices are defined. Black dots
431 indicate that the trends were above the 95% confidence level.

432 Figure 4. Variations in HD_{NC} (in black) and the SST_{P} (unit: $^{\circ}\text{C}$; a, red), SST_{A} (unit: $^{\circ}\text{C}$; b, blue), Snowc (unit: $\%$; c, yellow),
433 and Soilw (unit: mm ; d, green) indices and the HD_{NC} values fitted by the MLR model by the above four factors (unit: days; e,
434 purple) from 1979 to 2018. Thick lines indicate 5-year running averaged time series. The rectangles and triangles indicate the
435 inflection points of HD_{NC} and the four indices, which were tested by the Mann-Kendall test.

436 Figure 5. Composite of the simulated HD_{NC} caused by the four external forcing factors (Favor Years minus Unfavor Years).
437 The circles and crosses represent the original and detrended sequences, respectively.

438

441 **Table 1.** Correlation coefficients (CCs) between HD_{NC} and the SST_P , SST_A , $Snowc$ and $Soilw$ indices after detrending and the
 442 trends of the SST_P , SST_A , $Snowc$ and $Soilw$ indices for the periods 1991–2010 and 2010–2018. CC_1 , CC_2 , and CC_3 represent
 443 the correlation coefficients from 1979 to 2018, 1979 to 2010 and 2010 to 2018, respectively. “***” indicates that the CC was
 444 above the 99% confidence level, “**” indicates that the CC was above the 95% confidence level, and “*” indicates that the
 445 CC was above the 90% confidence level.

446

| | CC with HD_{NC} | Trend / 10yr | |
|---------|--------------------|--------------|-------------|
| | | 1991–2010 | 2010–2018 |
| SST_P | $CC_1 = 0.67$ *** | -0.20 °C*** | 1.99 °C*** |
| | $CC_2 = 0.39$ ** | | |
| | $CC_3 = 0.66$ *** | | |
| SST_A | $CC_1 = -0.64$ *** | 0.55 °C*** | -0.52 °C*** |
| | $CC_2 = -0.54$ *** | | |
| | $CC_3 = -0.61$ *** | | |
| $Snowc$ | $CC_1 = 0.54$ *** | -1.79% ** | 28.35% *** |
| | $CC_2 = 0.46$ *** | | |
| | $CC_3 = 0.53$ *** | | |
| $Soilw$ | $CC_1 = -0.60$ *** | 38.78mm*** | -51.81mm*** |
| | $CC_2 = -0.30$ * | | |
| | $CC_3 = -0.66$ *** | | |

447

448 **Table 2.** The contribution rate of fitted HD_{NC} and each external forcing factor to the trend of HD_{NC} in P1 and P2,
 449 respectively.

| | Fitted HD_{NC} | SST_P | SST_A | $Snowc$ | $Soilw$ |
|----|------------------|---------|---------|---------|---------|
| P1 | 112.2% | 23.3% | 43.9% | 4.5% | 40.7% |
| P2 | 72.3% | 41.9% | 7.5% | 12.9% | 10.0% |

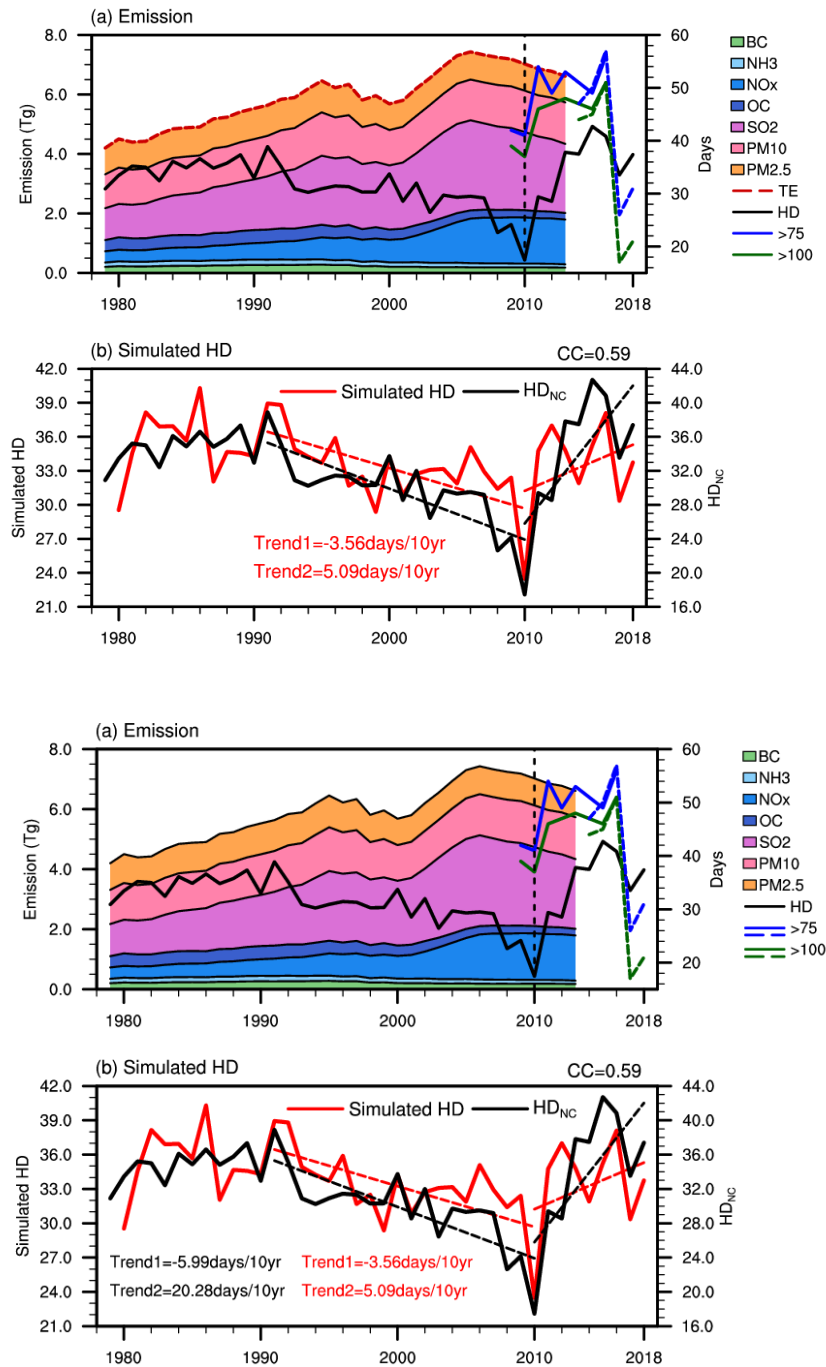
450

451

452

453

454

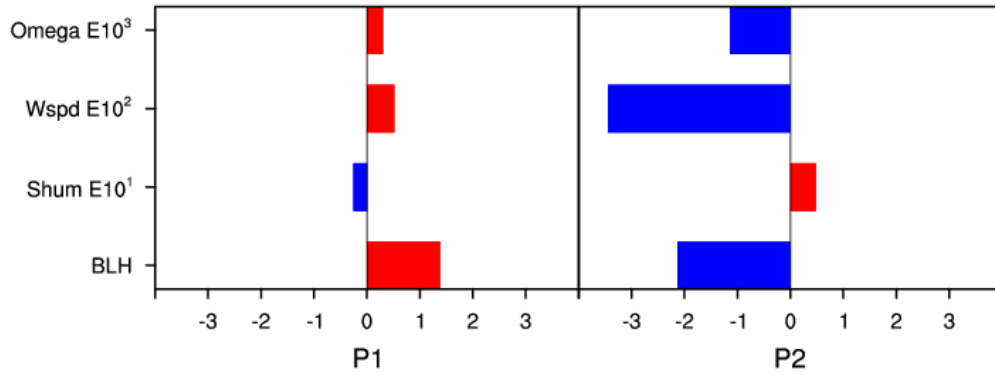


456

457

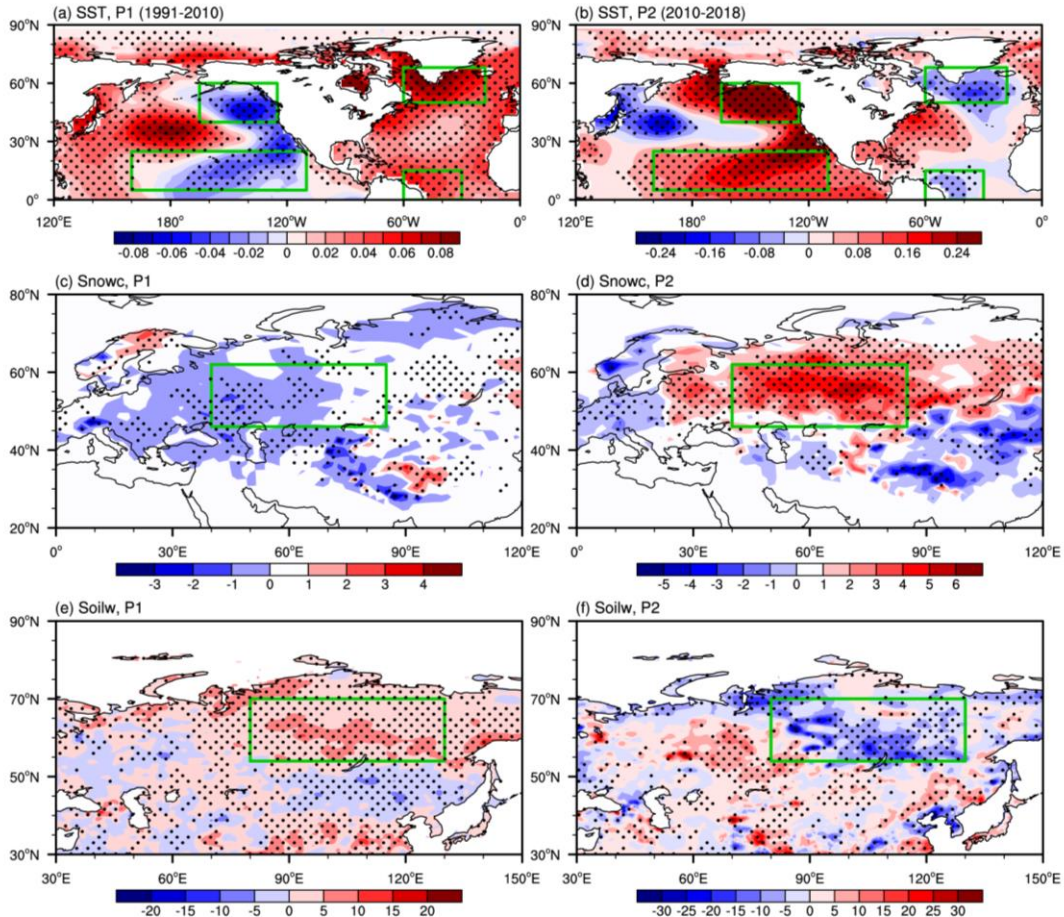
458 **Figure 1.** (a) Variations in the December-January emissions (unit: Tg) of black carbon (BC), ammonia (NH₃), nitrogen oxide
 459 (NO_x), organic carbon (OC), sulfur dioxide (SO₂), PM₁₀ and PM_{2.5} over North China from 1979 to 2013 and the variation in
 460 HD_{NC} from 1979 to 2018 (black solid line). The red dashed line represents the total emissions of the seven pollutants. The blue
 461 and green solid (dashed) lines indicate the number of days when the hourly PM_{2.5} concentrations in a day exceeded 75 $\mu\text{g m}^{-3}$
 462 and 100 $\mu\text{g m}^{-3}$, respectively, from 2009 to 2016 (2014 to 2018) using [Beijing \(North China\)](#) observed data from the US
 463 embassy (China National Environmental Monitoring Centre). (b) Temporal evolutions of HD_{NC} (in black), simulated haze

464 days (unit: days; red) in NC. The dashed lines denote linear regressions for 1991–2010 (P1) and 2010–2018 (P2). The black
 465 and red Trend 1 and Trend 2 represent the linear trends of the observed and simulated haze days in P1 and P2, respectively.



466
 467 **Figure 2.** Area-averaged linear trends of the BLH (unit: m/yr), specific humidity (unit: \%/10 yr), surface wind speed (unit: m
 468 $\text{s}^{-1}/10^2 \text{ yr}$) and omega (unit: $\text{pascal s}^{-1}/10^3 \text{ yr}$) over NC in early winter for the periods 1991–2010 (P1) and 2010–2018 (P2).
 469 All datasets were 5-year running averages before calculating the trends.

470



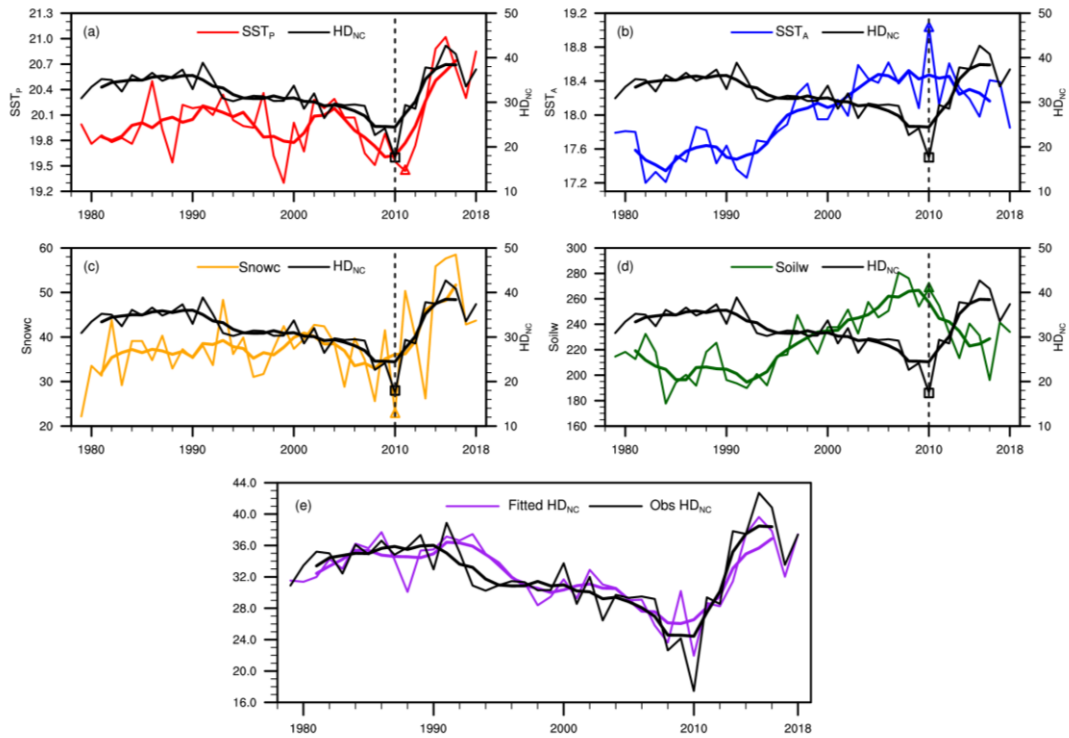
471
 472 **Figure 3.** Linear trends of the Pacific and Atlantic SST (unit: $^{\circ}\text{C}/\text{yr}$; a, b), Eurasian snow cover (unit: \%/yr ; c, d), and central
 473 Siberian soil moisture (unit: mm/yr ; e, f) for the periods 1991–2010 (P1) and 2010–2018 (P2). All datasets were 5-year

474 running averages before calculating the trends. The green boxes represent the regions where the four indices are defined.

475 Black dots indicate that the trends were above the 95% confidence level.

476

477



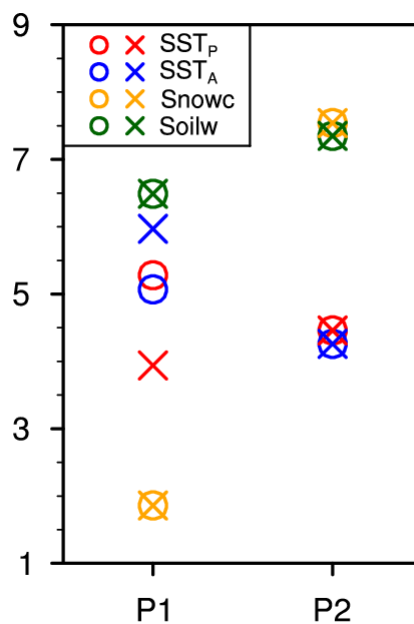
478

479 **Figure 4.** Variations in HD_{NC} (in black) and the SST_P (unit: °C; a, red), SST_A (unit: °C; b, blue), Snowc (unit: %; c, yellow),

480 and Soilw (unit: mm; d, green) indices and the HD_{NC} values fitted by the MLR model by the above four factors (unit: days;

481 e, purple) from 1979 to 2018. Thick lines indicate 5-year running averaged time series. The rectangles and triangles indicate

482 the inflection points of HD_{NC} and the four indices, which were tested by the Mann-Kendall test.



483

484 **Figure 5.** Composite of the simulated HD_{NC} caused by the four external forcing factors (Favor Years minus Unfavor Years).
485 The circles and crosses represent the original and detrended sequences, respectively.
486